

Research Article

Identification of Ten-Gene Related to Lipid Metabolism for Predicting Overall Survival of Breast Invasive Carcinoma

Zhixing Wang and Fan Wang 

Medical College, Jiangsu Vocational College of Medicine, YanCheng 224000, Jiangsu, China

Correspondence should be addressed to Fan Wang; 12154@jsmc.edu.cn

Received 23 May 2022; Revised 10 June 2022; Accepted 17 June 2022; Published 11 July 2022

Academic Editor: Mohammad Farukh Hashmi

Copyright © 2022 Zhixing Wang and Fan Wang. This is an open access article distributed under the Creative Commons Attribution License, which permits unrestricted use, distribution, and reproduction in any medium, provided the original work is properly cited.

Background. Predicting the risk of poor prognosis of breast cancer is crucial to treating breast cancer. This study investigated the prognostic assessment of 10 lipid metabolism-related genes constructed as breast cancer models based on this study. **Methods.** The TCGA database was used to obtain clinical information and expression data of breast cancer patients, and GSEA analysis and univariate and multivariate Cox proportional risk regression models were performed to identify lipid metabolism genes closely associated with overall survival (OS) of breast cancer patients and to construct a prognostic risk score model based on lipid metabolism gene markers. The Kaplan–Meier method was used to analyze the survival status of patients with high and low-risk scores, and ROC curves assessed the accuracy of this risk score. Finally, the relationship between this risk score and clinicopathological characteristics of BRCA was analyzed in a stratified manner, and the validity of this risk score as an independent prognostic factor was determined using univariate and multivariate Cox regression analyses. **Results.** One hundred and forty-four differentially expressed lipid metabolism-related genes were identified in cancer and paracancerous tissues in BRCA, 21 of which were associated with overall survival (OS) in BRCA ($P < 0.05$). Univariate and multivariate Cox analyses revealed that age, grade, and risk score were independent prognostic factors for BRCA. Multivariate Cox regression analysis further identified APOL4, NR1H3, SLC25A5, APOL3, OSBPL1A, DYNLT1, IMMT, MAP2K6, ZDHHC8, and RAB2A lipid metabolism-related genes as independent prognostic markers for BRCA. A prognostic risk score model was developed by labeling lipid metabolism genes with these 10 genes, and patients with BRCA with high-risk scores in the model sample had significantly worse OS than those with low-risk ($P < 0.01$). The ROC curve area (AUC) of this risk score model was 0.712. **Conclusion.** By mining the TCGA database, we identified 10 lipid metabolism-related genes APOL4, NR1H3, SLC25A5, APOL3, OSBPL1A, DYNLT1, IMMT, MAP2K6, ZDHHC8, and RAB2A, which are closely related to the prognosis of BRCA patients, and constructed a prognostic risk scoring system based on 10 lipid metabolism genes tags.

1. Background

According to statistics, in 2020, for the first time, breast cancer in women will overtake lung cancer as the most common cancer worldwide [1]. Currently, the main treatments for breast cancer include surgery, chemotherapy, radiotherapy, and targeted therapy, but all have varying degrees of side effects that affect the prognosis of patients [1]. Therefore, predicting the risk of poor prognosis in breast cancer is crucial for breast cancer treatment. Lipids are widely distributed in cellular organelles and are a crucial part of all membranes; they form the basic structure of

membranes, signal molecules, and energy sources [2, 3]. There is growing evidence that the lipid metabolism is largely reprogrammed in cancer [4, 5] and that lipid production in human cancers is strongly upregulated to meet the demands of increased membrane biogenesis [6, 7]. Most types of cancers use lipids and cholesterol to meet their unlimited energy requirements [8]. Increased lipid uptake, storage, and lipogenesis have been shown to occur in various cancers and contribute to rapid tumor growth [9]. Based on this background, this study used the TCGA database to obtain clinical information and expression data of breast cancer patients, identified lipid metabolism genes that are

closely associated with overall survival (OS) of breast cancer patients, and constructed a prognostic risk scoring system based on 10 lipid metabolism gene tags, which provides new targets for diagnosis and treatment of breast cancer and can promote human understanding of the pathogenesis of breast cancer and improve. It can promote human understanding of the pathogenesis of breast cancer and improve diagnosis and treatment.

2. Methods

2.1. Collection of Genetic and Clinical Data. Breast cancer patients' clinical data and mRNA expression profiles were downloaded from the TCGA database (<https://portal.gdc.cancer.gov/>). The selection criteria were set as the primary cancer site was the breast, the project name was TCGA-BRCA, the expression data type was HTSeq-FPKM, the data type was a transcript, and the experimental method was RNA-Seq technology. This data matrix contains 1109 breast cancer patients and 113 healthy controls. The dataset of 8 genes related to the lipid metabolism was downloaded from the GSEA official website (<https://www.gsea-msigdb.org/gsea/downloads.jsp>).

2.2. Gene Set Enrichment Analysis. The eight downloaded datasets were enriched and analyzed with GSEA 4.1.0, and validated lipid metabolism-related gene datasets with standardized $P < 0.05$ were screened separately. Lipid metabolism genes and their expressions were extracted from these 8 datasets, screened for $P < 0.05$ differential analysis using the limma package, and combined the differential gene expression and survival data.

2.3. Construction of a Prognostic Model for Lipid Metabolism. Univariate Cox regression analysis was applied to identify lipid metabolism-related genes associated with overall survival, and then, multivariate Cox regression was performed to screen out the prognosis-related lipid metabolism genes and obtain the hazard ratio (HR). The screened lipid metabolism genes were then classified into hazard ($HR > 1$) and protective ($0 < HR < 1$) types. A prognostic risk score model was constructed according to the linear combination of expression levels, and the regression coefficients obtained by multivariate Cox regression analysis were weighted with the following risk parameter formula: risk parameter = $\sum (\beta_n \times \text{expression of gene } n)$.

Using the survival package in R 4.0.2, a prognostic model of the lipid metabolism in breast cancer with minimal AIC value was constructed by multifactorial COX regression, and the risk values of patients were output. The survival curves of the 2 groups were plotted according to the median value divided into 2 groups of high and low risks, and the risk curves were plotted using ROC curves to judge the validity of the model diagnosis.

2.4. Lipid Metabolism-Related Features Are Independent Prognostic Factors for Breast Cancer. Univariate and

multivariate Cox regression analyses and data stratification analyses were performed to assess whether risk scores were independent of clinical characteristics. $P < 0.05$ was considered statistically significant.

2.4.1. Mutation and Difference Analysis of Model Gene. Mutations in model genes were analyzed using the online network (<https://www.cbioportal.org/>), and breast cancer samples were selected from the TCGA dataset to analyze the frequency and type of mutations in lipid metabolism genes of tumors in the prognostic model. All steps were performed according to the cBioPortal instructions.

2.5. Statistical Analysis. Using Kaplan–Meier survival curves and the log-rank method (Log-rank), the accuracy of risk parameters was estimated. Multivariate Cox analyses were then performed to test whether risk parameters were independent of other clinical characteristics, and all statistical analyses were performed using R 4.0.2, with $p < 0.05$ being statistically significant.

3. Results

3.1. Enrichment Analysis of Lipid Metabolism in Thyroid Carcinoma. The clinical data and mRNA expression datasets of 1109 BRCA patients were obtained from The Cancer Genome Atlas (TCGA). After screening 8 datasets, 5 datasets were finally found to be eligible, and GSEA analysis of 1494 genes involved in lipid metabolic processes revealed that most of these genes were more active in the tumor samples. Values (P), where $FDR < 0.1$ and $P < 0.05$, were used to screen eligible gene sets, and FDR was performed for lipid metabolism gene subset size and multiple hypothesis test correction (Figure 1). GSEA determined that KEGG_ARACHIDONIC_ACID_METABOLISM, KEGG_ETHER_LIPID_METABOLISM, KEGG_GLYCEROLIPID_METABOLISM, KEGG_GLYCEROPHOSPHOLIPID_METABOLISM, and WP_LIPID_METABOLISM_PATHWAY are five sets of lipid metabolism-related genes upregulated in BRCA.

3.2. Lipid Metabolism Genes Related to the Prognosis of Thyroid Carcinoma. Univariate Cox regression analysis was performed on the expression of lipid metabolism-related genes in eight genomes in BRCA to identify prognostically relevant differentially expressed genes for the lipid metabolism. The data showed that the expression of 21 differentially expressed lipid metabolism-related genes was associated with OS in patients with BRCA ($P < 0.05$) (Table 1). Next, multivariate Cox regression analysis was performed to identify further 10 lipid metabolism-related genes APOL4, NR1H3, SLC25A5, APOL3, OSBPL1A, DYNLT1, IMMT, MAP2K6, ZDHHC8, and RAB2A as independent prognostic markers for BRCA, with SLC25A5, DYNLT1, and HRs for IMMT and RAB2A identified. With HRs greater than 1 for IMMT and RAB2A, risk phenotypes are with low patient survival (Table 2).

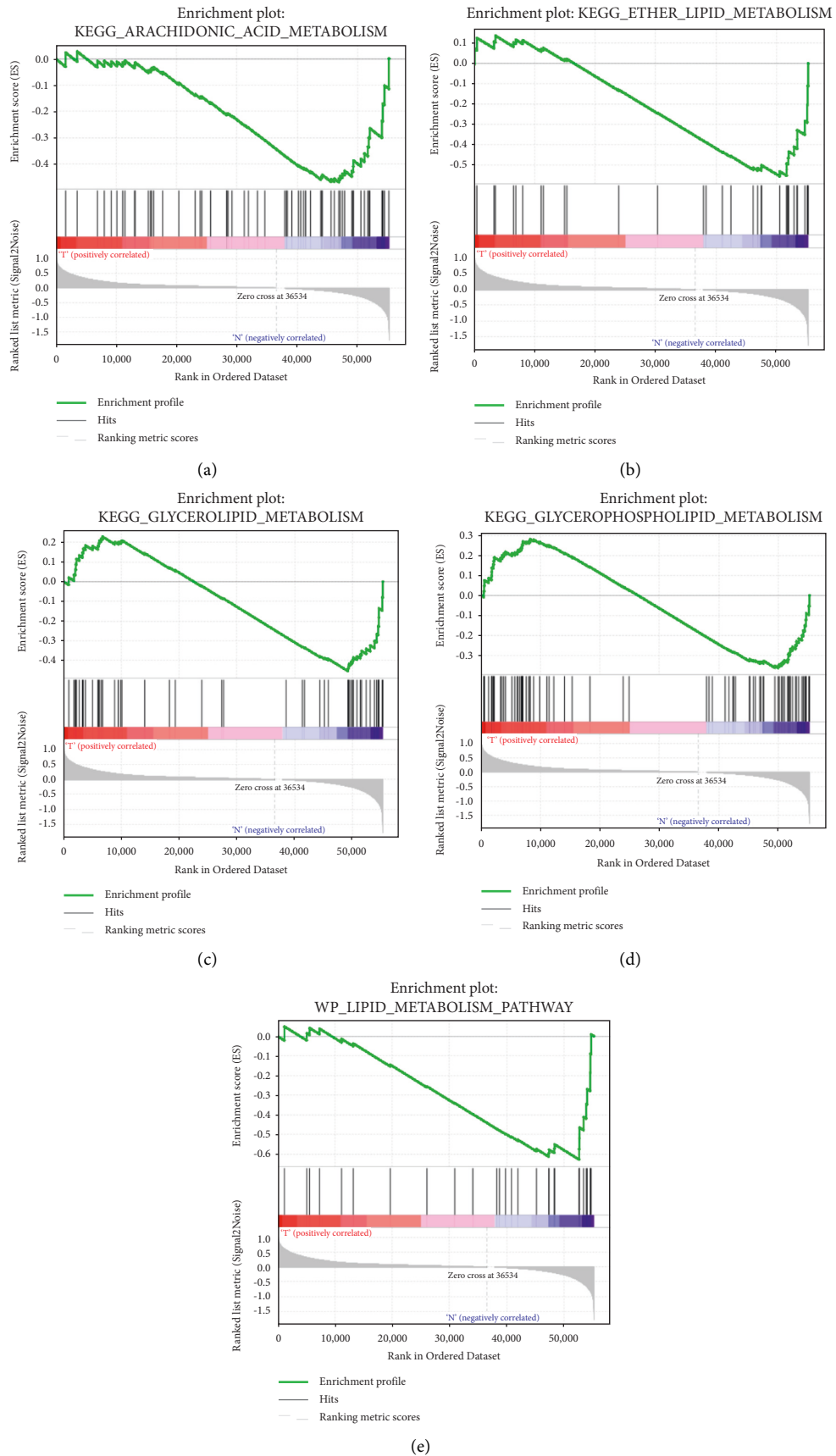


FIGURE 1: Enrichment analysis of lipid metabolism gene set. (a) $P = 0.003$, KEGG_ARACHIDONIC_ACID_METABOLISM. (b) $P = 0.005$, KEGG_ETHER_LIPID_METABOLISM. (c) $P = 0.021$, KEGG_GLYCEROLIPID_METABOLISM. (d) $P = 0.037$, KEGG_GLYCEROPHOSPHOLIPID_METABOLISM. (e) $P = 0.013$, WP_LIPID_METABOLISM_PATHWAY.

TABLE 1: 21 univariate Cox regression-associated lipid metabolism genes in breast cancer.

Gene	HR	HR.95L	HR.95H	Cox P value
APOL4	0.900877879	0.834348061	0.972712697	0.00765844
NR1H3	0.919241179	0.865931412	0.975832881	0.005735271
SLC25A5	1.001960965	1.000317045	1.003607587	0.019370037
APOL3	0.948868181	0.913186198	0.985944408	0.007279521
OSBPL1A	0.959529209	0.923596388	0.996860007	0.03388302
DYNLT1	1.017520083	1.005999394	1.029172708	0.002794158
HSPA9	1.009104615	1.004457297	1.013773434	0.000118927
SLC35A2	1.025997849	1.009627085	1.042634059	0.001763323
ENPP6	0.400790856	0.165340628	0.971529573	0.042980469
IMMT	1.021791143	1.00438895	1.03949485	0.013907542
GBP2	0.980967649	0.967334692	0.994792739	0.007120906
MAP2K6	0.767586959	0.616910246	0.955065576	0.017677113
ZDHHC8	0.910449729	0.845440542	0.980457723	0.013060524
HSPA4	1.010302771	1.001638957	1.019041523	0.019666949
KDEL2	1.005368525	1.001401791	1.009350973	0.007943869
YWHAB	1.005431653	1.002346635	1.008526165	0.000550569
DENND5A	0.948306241	0.899822755	0.999402073	0.047445508
RAB2A	1.01409836	1.00636175	1.021894447	0.000339738
WLS	0.980395937	0.962721035	0.998395337	0.032926553
KDEL1	1.003917855	1.000416053	1.007431914	0.028286843
ZDHHC9	1.032053594	1.012770657	1.051703674	0.001043034

TABLE 2: 10 multivariate Cox regression-associated lipid metabolism genes in breast cancer.

Id	Coefficient	HR
APOL4	-0.053646743	0.947766852
NR1H3	-0.048036694	0.953098814
SLC25A5	0.001753325	1.001754863
APOL3	-0.030663112	0.969802232
OSBPL1A	-0.045680466	0.95534718
DYNLT1	0.010606609	1.010663058
IMMT	0.017937573	1.018099418
MAP2K6	-0.252082595	0.777180544
ZDHHC8	-0.056161117	0.945386806
RAB2A	0.009273916	1.009317052

3.3. Prognostic Model of Lipid Metabolism in Thyroid Carcinoma. A prognostic model consisting of APOL4, NR1H3, SLC25A5, APOL3, OSBPL1A, DYNLT1, IMMT, MAP2K6, ZDHHC8, and RAB2A was constructed by multifactorial COX regression based on the risk value = APOL4 expression \times 0.9478 + NR1H3 expression \times 0.9531 + SLC25A5 expression \times 1.0018 + APOL3 expression \times 0.9698 + OSBPL1A expression \times 0.9553 + DYNLT1 expression \times 1.0107 + IMMT expression \times 1.0181 + MAP2K6 expression \times 0.7772 + ZDHHC8 expression \times 0.9454 + RAB2A expression \times 1.0093 and the value was calculated. According to their median, the patients were then divided into 2 groups of high and low risks, with 545 breast cancer samples in the high-risk group and 545 breast cancer samples in the low-risk group. The prognosis of the high and low-risk groups was significantly different ($P < 0.01$), as shown by the survival curves (Figure 2(a)). The ROC curve showed that the AUC value was 0.712, indicating the model's predictive value (Figure 2(b)).

3.4. Risk Curve. Risk parameters were calculated for each patient, and the patients were divided into high and low-risk

groups using the median. The distribution of patients' risk scores (Figure 3(a)) and survival status (Figure 3(b)) are shown. In addition, the heat map shows the expression of the 10 mRNAs (Figure 3(c)). As patients' risk scores increased, the proportion of patients who died gradually increased, and the survival time was significantly shortened. Meanwhile, SLC25A5, DYNLT1, IMMT, and RAB2A were highly expressed in the high-risk group.

3.5. Independent Prognostic Analysis of Univariate and Multivariate. Comparing the prognostic value of risk parameters with clinicopathological parameters by univariate and multifactorial analyses showed that gender was not a good predictor of prognosis in breast cancer patients. In contrast, the prognostic model studied here, age, grading, and risk score, could effectively assess the prognosis of patients with a p value less than 0.01, showing a significant prognostic value (Figure 4).

3.6. Mutation and Difference Analysis of Model Gene. Alterations in 10 risk genes were evaluated by analyzing 996 BRCA samples from the cBioPortal database

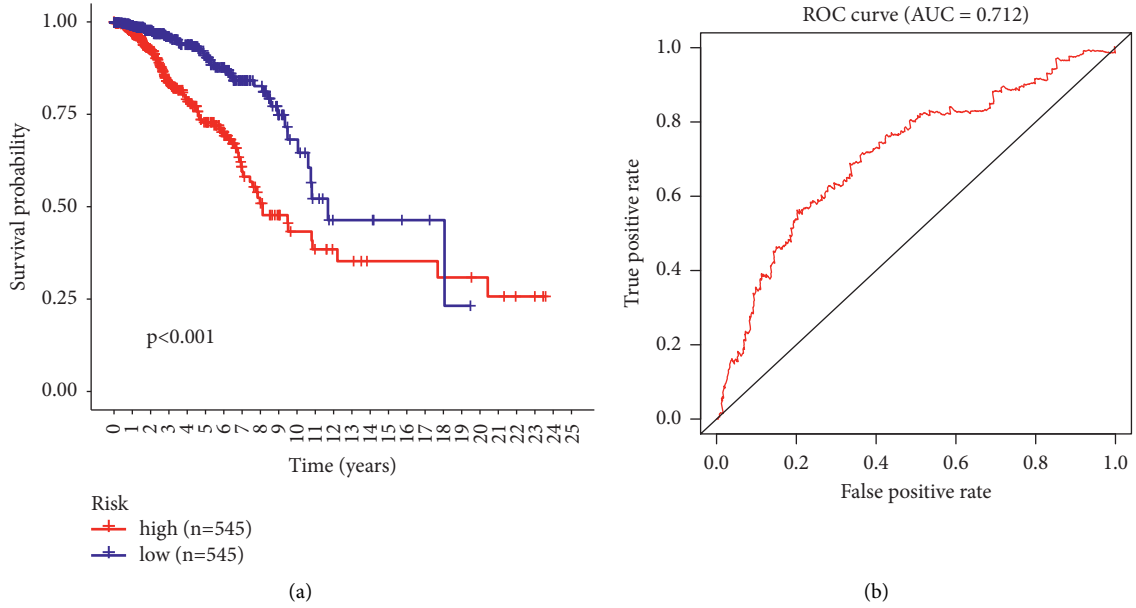


FIGURE 2: Survival analysis of the lipid metabolism prognostic model with ROC curves.

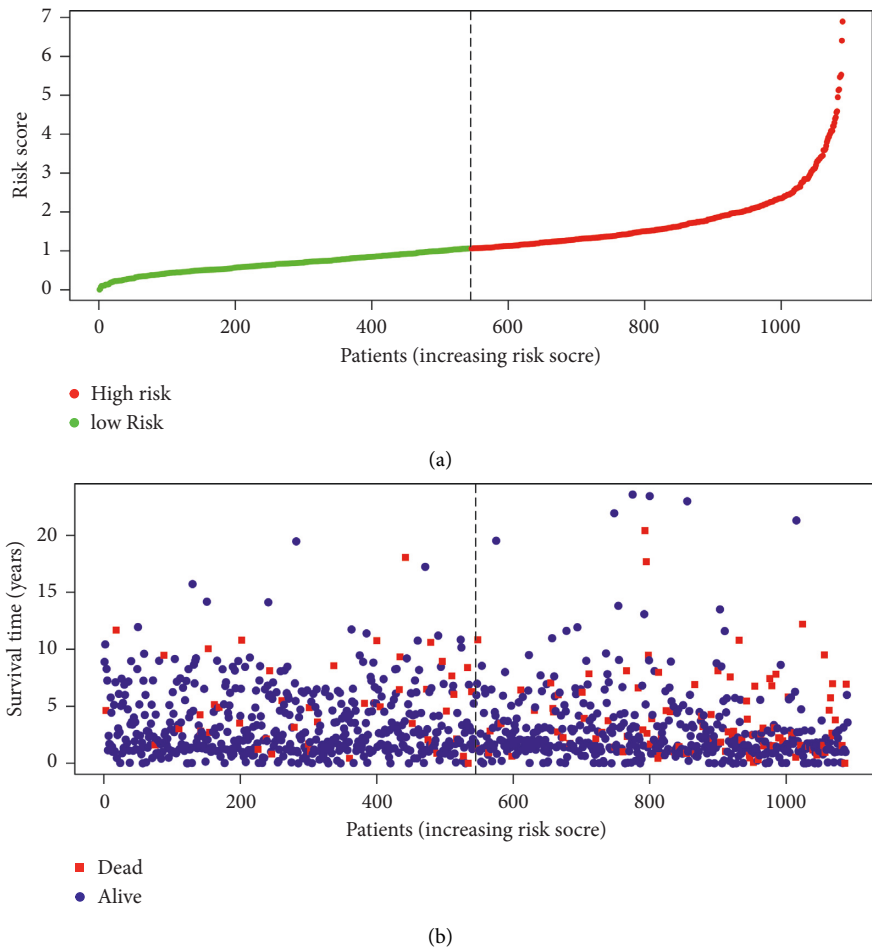
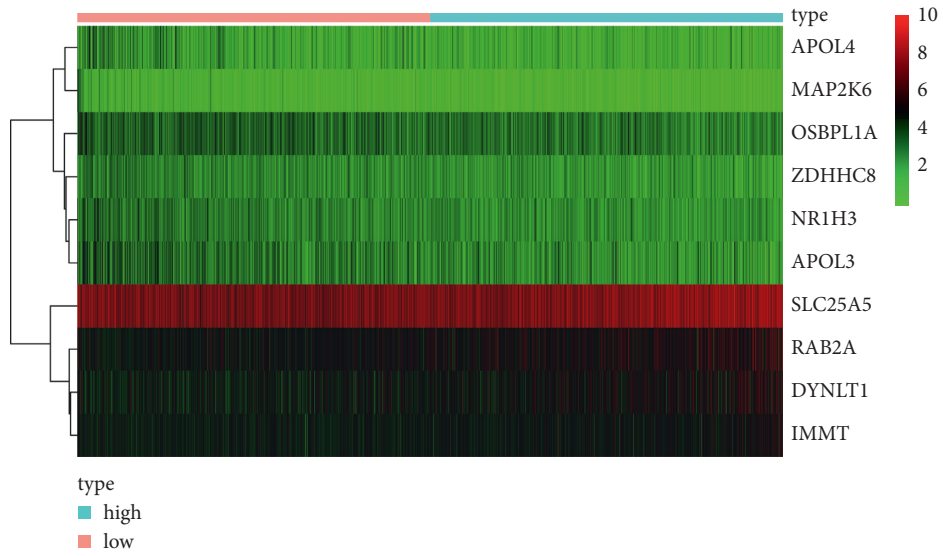


FIGURE 3: Continued.



(c)

FIGURE 3: Risk curve.

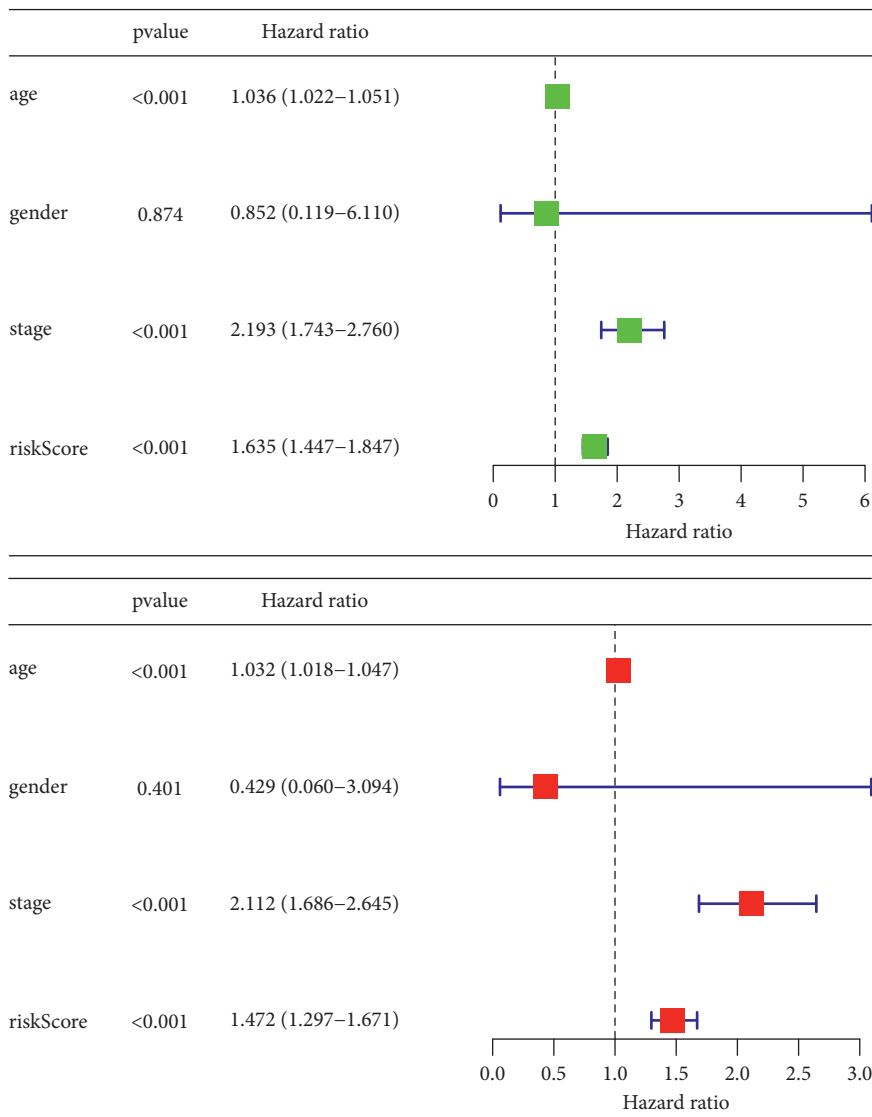
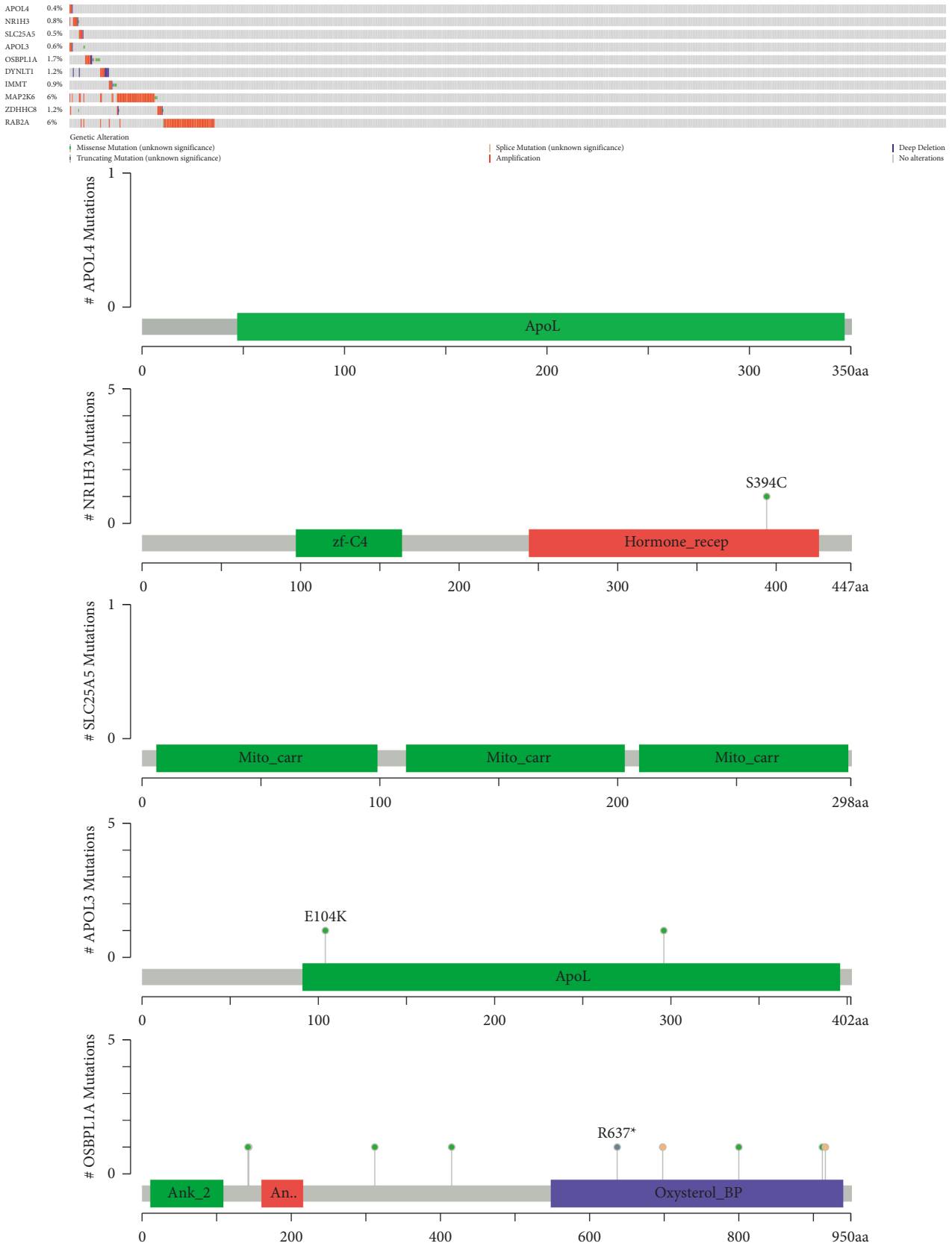


FIGURE 4: Independent prognostic analysis.



(a)
FIGURE 5: Continued.

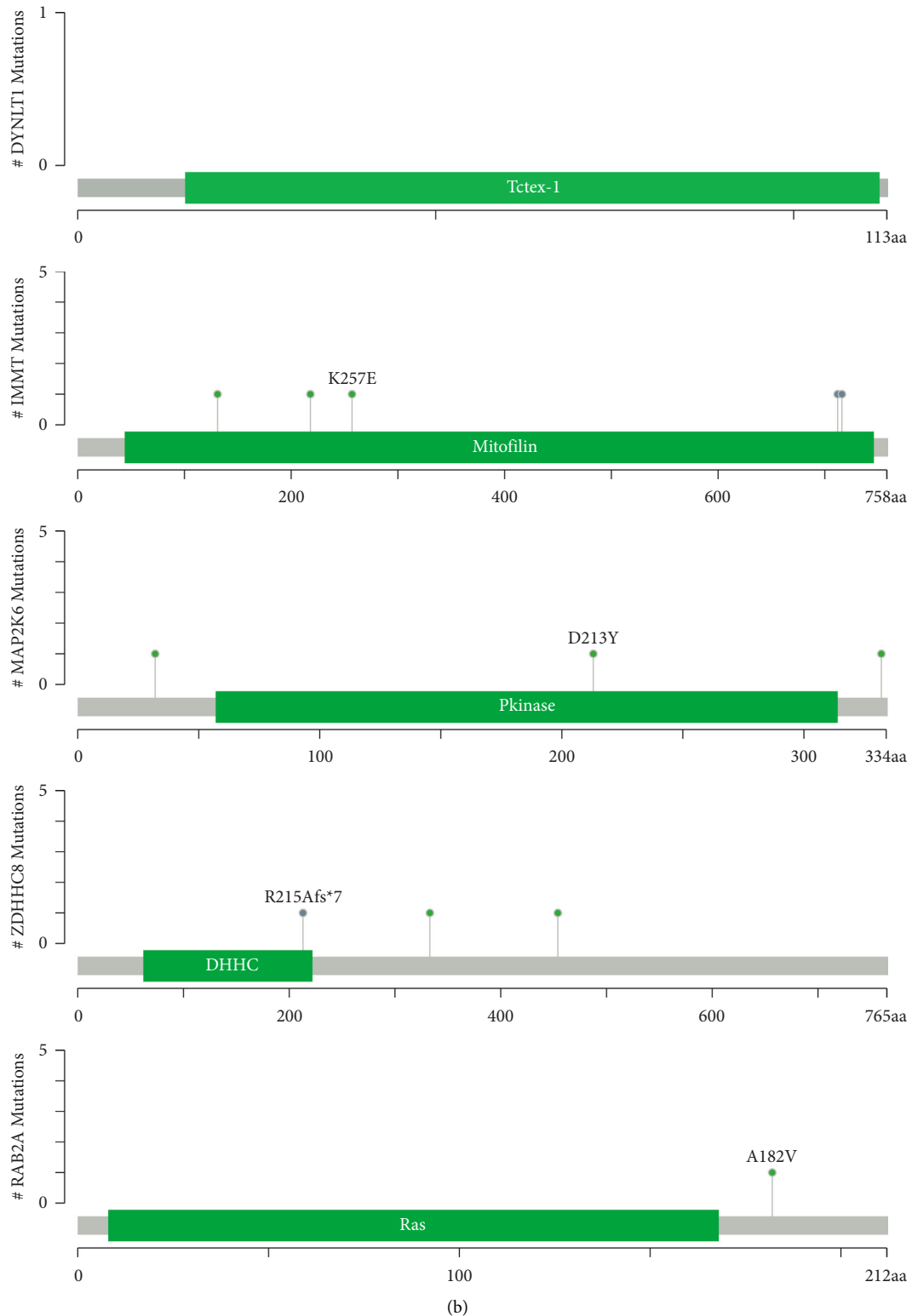
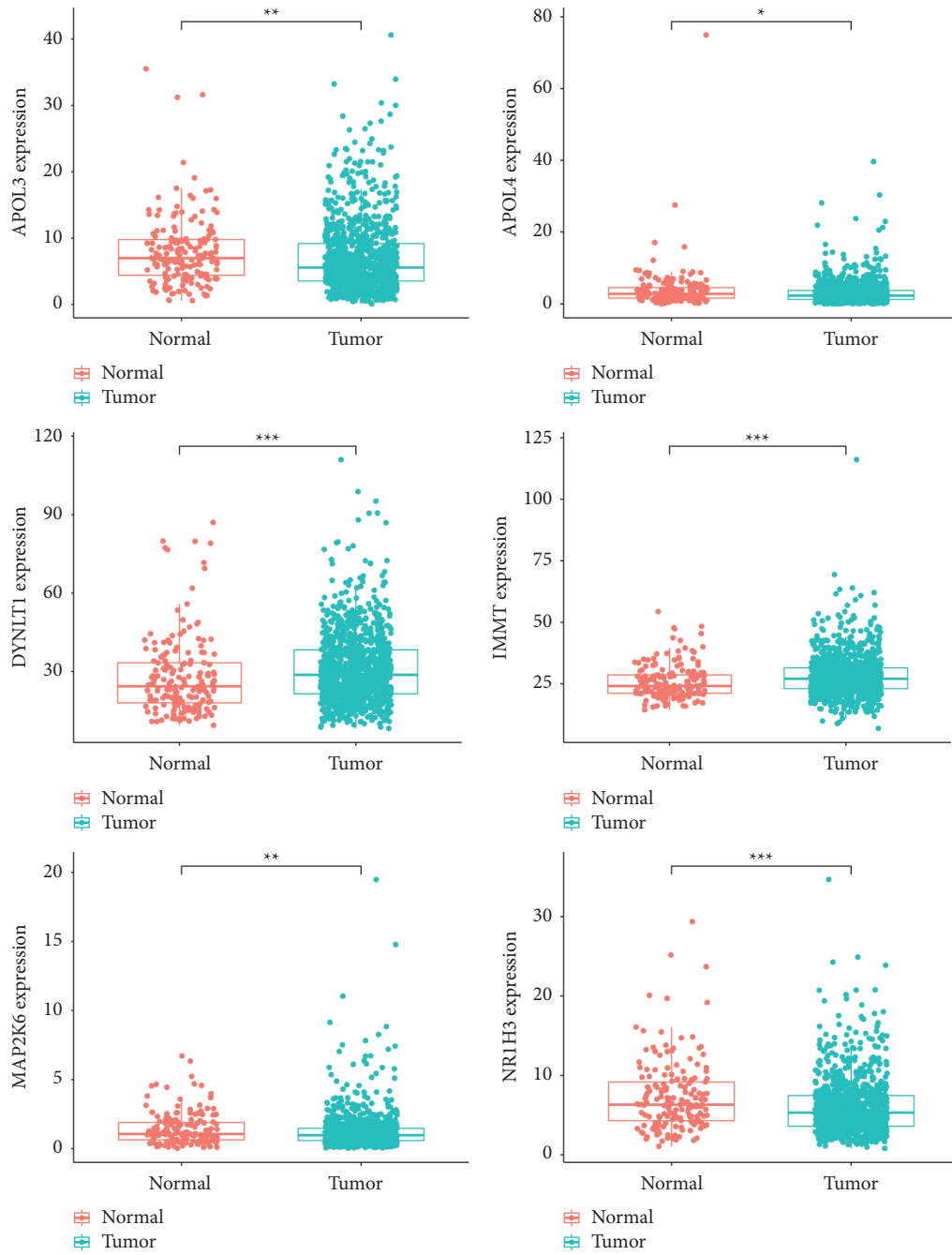


FIGURE 5: Mutations in prognostic model genes.

(<https://cbiportal.org>). The APOL4 gene was altered in 0.4% of cases, showing amplification mutations and deep deletions. NR1H3 gene was altered in 0.8% of cases, showing amplification mutations, deep deletions, and missense mutations. The DYNLTI gene was altered in 1.2% of cases, showing amplification mutations and deep deletions. The SLC25A5 gene was altered in 0.5% of cases, showing

amplification mutations and deep deletions. APOL3 gene was altered in 0.6% of cases, showing amplification mutations, deep deletions, and missense mutations. The DYNLTI gene was altered in 1.2% of cases, showing amplification mutations and deep deletions. The IMMT gene was altered in 0.9% of cases,



(a)

FIGURE 6: Continued.

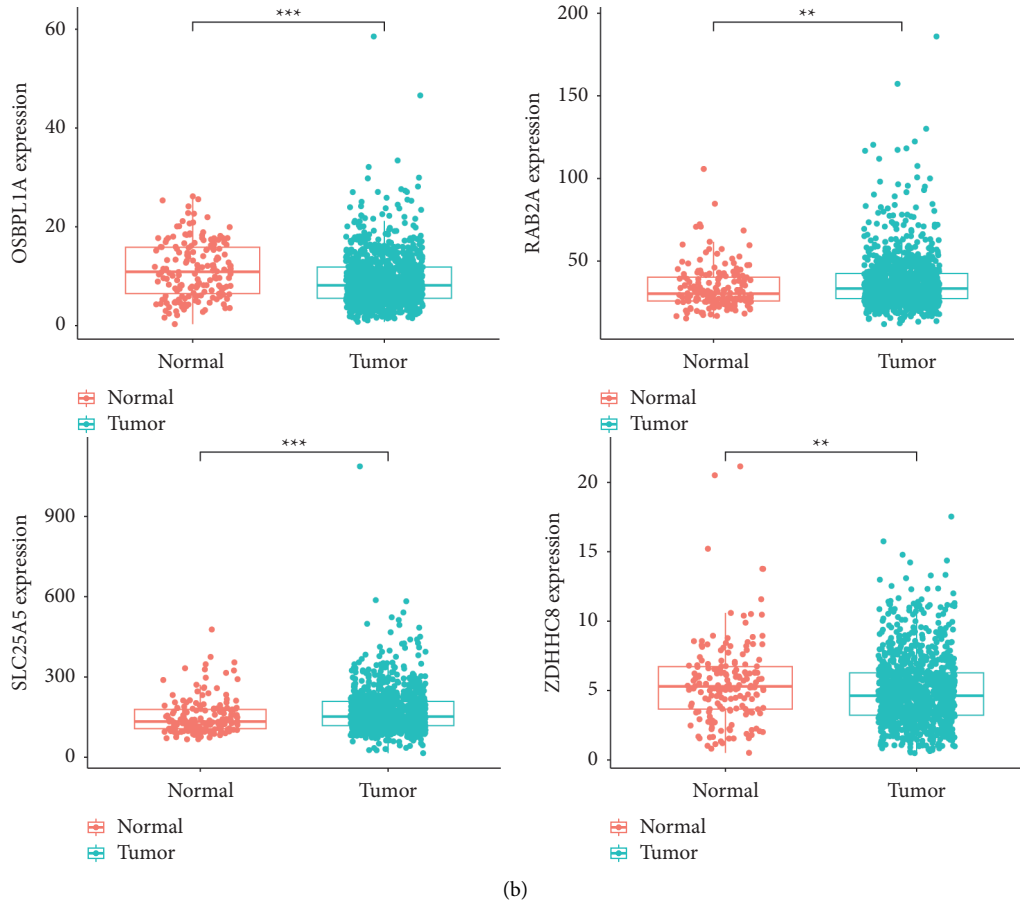


FIGURE 6: Differential analysis of prognostic model genes.

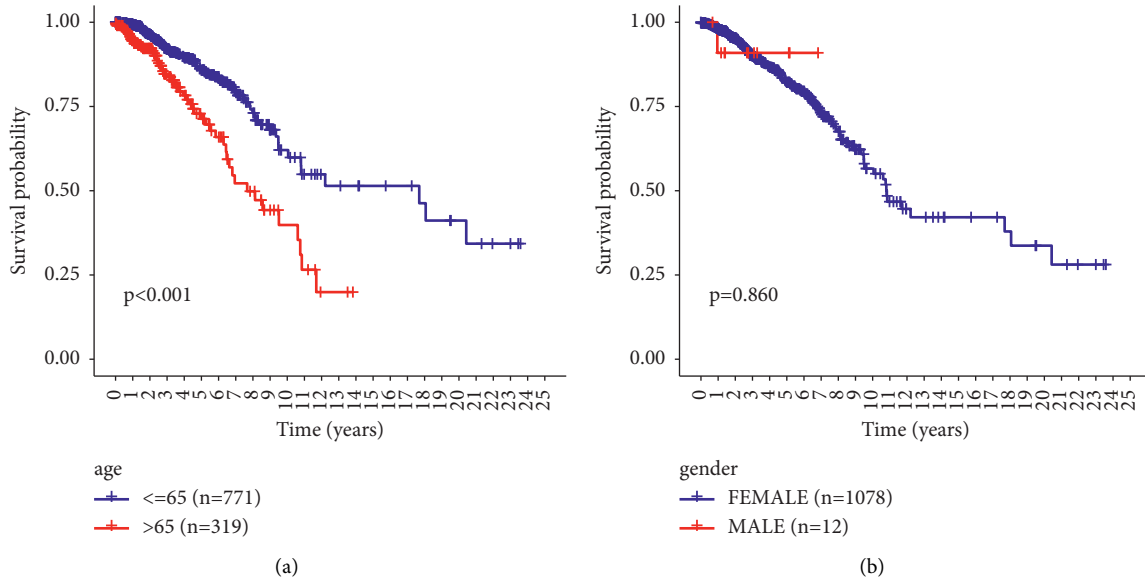


FIGURE 7: Continued.

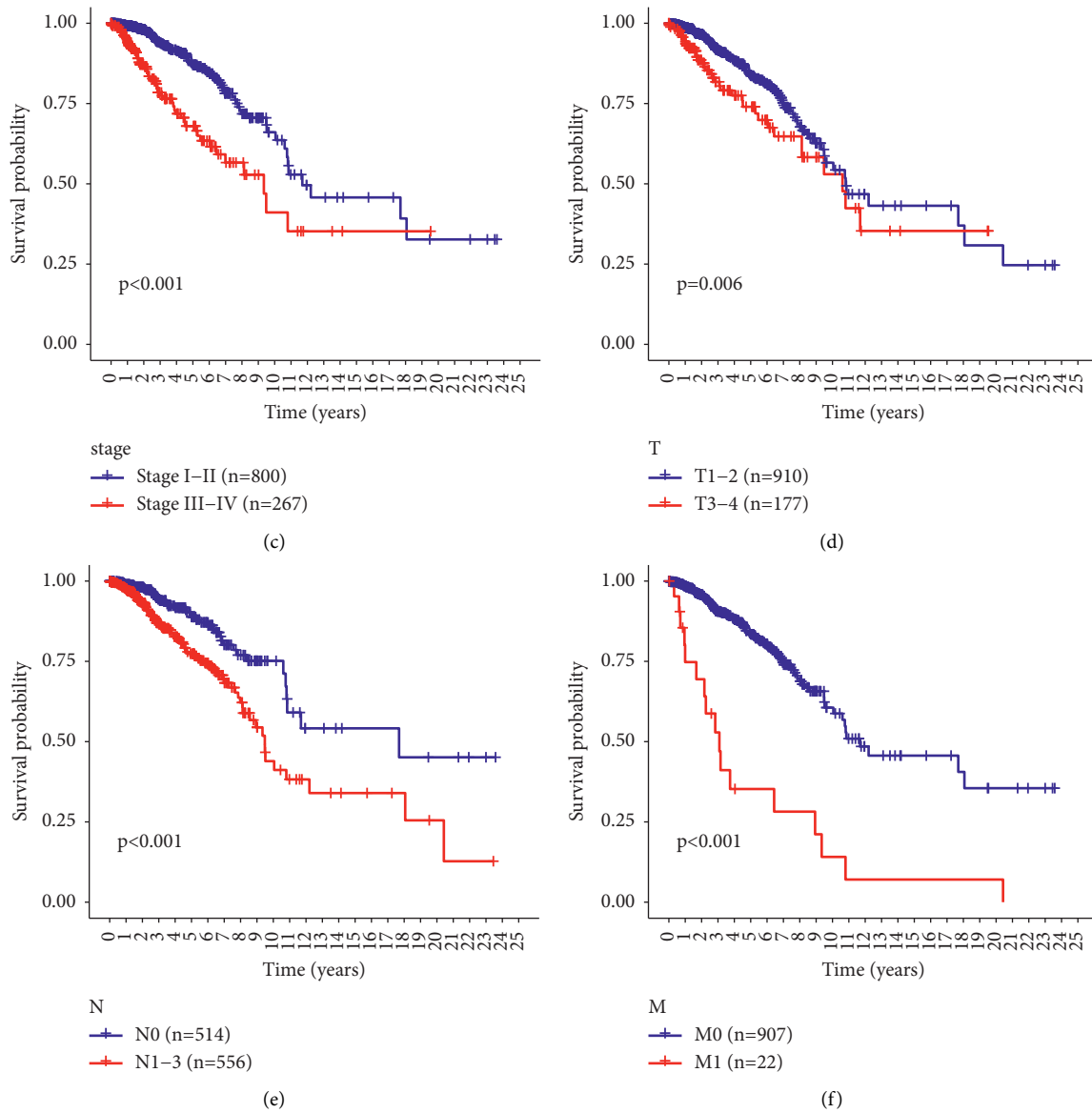


FIGURE 7: Relationship between risk score distribution and clinical parameters.

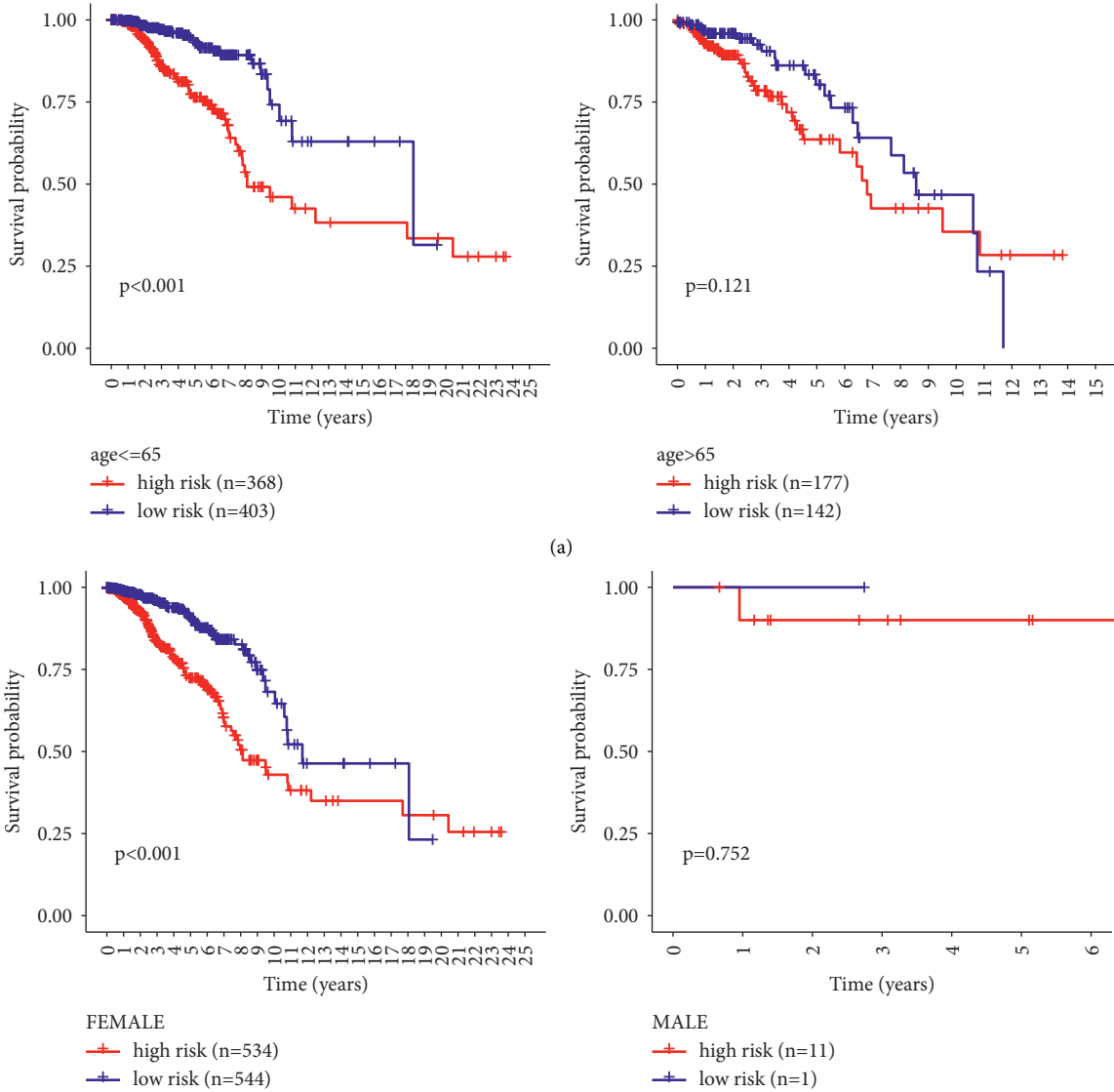
showing amplification mutations, deep deletions, truncation, and missense mutations. The ZDHHC8 gene was altered in 1.2% of cases with amplification mutations, deep deletions, truncation mutations, and missense mutations, and the MAP2K6 and RAB2A genes were altered in 6% of cases with amplification mutations and missense mutations (Figure 5).

The expression of APOL4, NR1H3, SLC25A5, APOL3, OSBPL1A, DYNLT1, IMMT, MAP2K6, ZDHHC8, and RAB2A was upregulated in both normal and tumor samples. P value for APOL3, MAP2K6, RAB2A, and ZDHHC8 was less than 0.05, a significant difference; DYNLT1, IMMT, NR1H3, OSBPL1A, and SLC25A5 had a P value less than 0.001, and the difference was highly significant (Figure 6).

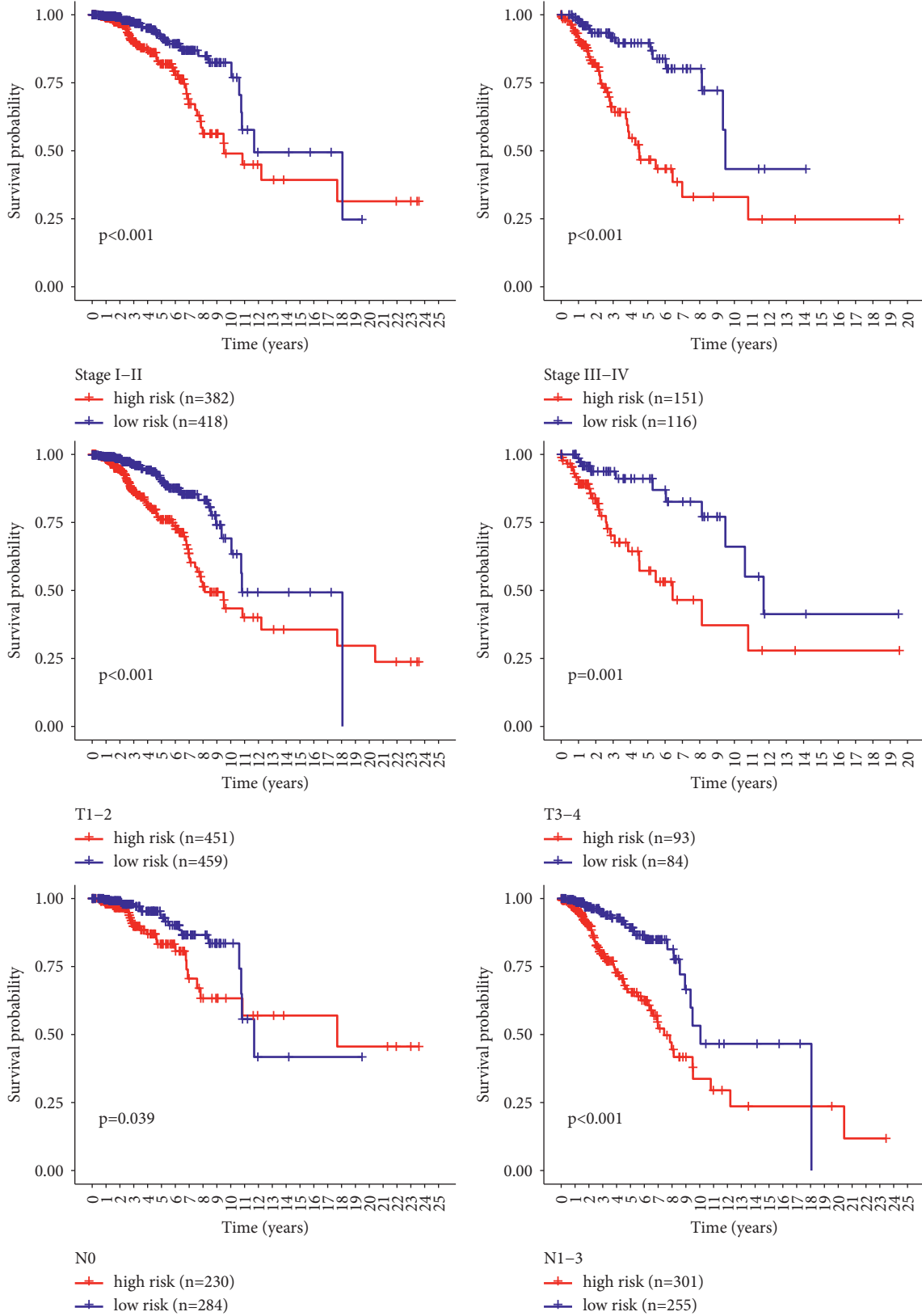
3.7. Model Validation of Survival Curves for Clinical Characteristics and Clinical Subgroups. Both univariate and multivariate Cox regression analyses of OS revealed several

clinicopathological parameters that predict BRCA survival, including age, grade, and risk score. We then validated these findings using Kaplan–Meier survival curves, which showed consistent results with age (Figure 7(a)), stage (Figure 7(c)), T-stage (Figure 7(d)), N-stage (Figure 7(e)), and M-stage (Figure 7(f)) being associated with poor prognosis. These results further confirm the reliability of the analysis.

Several clinical characteristics were evaluated by Kaplan–Meier analysis using log-rank tests to assess the predictive ability of BC patients. The results showed that the survival curve was not affected by the age >65 group (Figure 8(a)), and the prognosis of patients in the male subgroup with high-risk scores was not significant and could not be used to predict the prognosis of patients with BRCA (Figures 8(c) and 8(d)). However, when we divided BRCA patients into different subgroups according to TNM, the risk parameter could no longer be used as the M1 subgroup alone (Figure 8(l)), suggesting that this risk parameter is



(b)
FIGURE 8: Continued.



(c)

FIGURE 8: Continued.

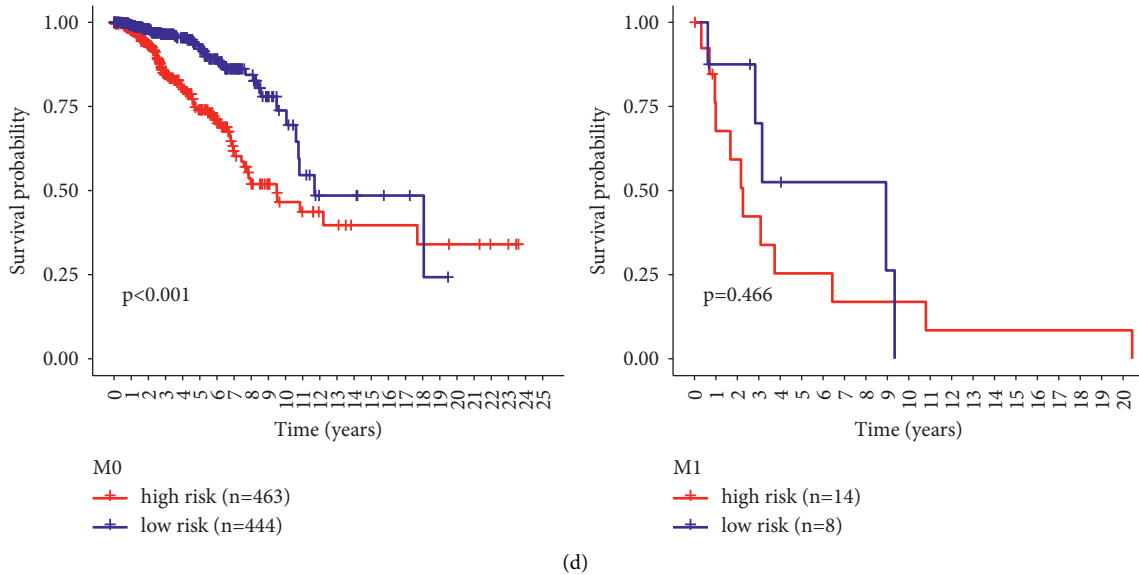


FIGURE 8: Kaplan–Meier curves to assess the prognostic value of risk parameters in patients grouped by clinical characteristics.

influenced by TNM staging BRCA patients, which needs to be further explored.

4. Conclusions

This study focused on assessing the prognosis of breast cancer by a model constructed from genes related to the lipid metabolism. It was shown that univariate and multifactorial Cox analyses showed that age, grade, and risk score were independent prognostic factors for BRCA, and the study was statistically significant. The results showed that *DYNLT1*, *IMMT*, *RAB2A*, and *SLC25A5* were unfavorable factors for breast cancer prognosis in the lipid metabolic pathway. *APOL3*, *APOL4*, *NR1H3*, *OSBPL1A*, *MAP2K6*, and *ZDHHC8* were protective genes for breast cancer prognosis.

It is well known that *APOL3*-controlled NCS-1 promotes cancer cell motility, metastatic spread, and survival. The reduction of $\pi(4)P$ observed in human breast cancer, where Golgi $\pi(4)P$ is a regulator of cell adhesion and invasive cell migration [10, 11]. *APOL1Δ* and *APOL3KO* foot cells can be responsible for this metastatic phenotype. *APOLs* are suspected to be involved in various cancers, including cervical, ovarian, breast, thyroid, bladder, prostate, and colorectal cancers [12–15]. It is known that *NR1H3* is involved in various metabolic functions such as cholesterol, fatty acid and glucose homeostasis, and steroidogenesis. The main physiological functions of *NR1H3* are maintenance of cholesterol levels, lipoprotein metabolism, and lipid synthesis, and at high cholesterol levels, *NR1H3* is a major transcriptional regulator involved in lipid metabolism gene synthesis [16–18]. Oxygen sterol binding protein-related protein 1 (*OSBPL1A*) is an intracellular lipid receptor and a member of the oxygen sterol binding protein (*OSBP*) family [19]. The familial loss-of-function mutation in *OSBPL1A* affects the first step of the reverse cholesterol transport process and is associated with a low HDL-C phenotype, suggesting that rare mutations in the *OSBPL*

gene may contribute to dyslipidemia [20]. *MAP2K6* is involved in various physiological and pathological processes, such as cell growth, development, division, and inflammatory responses. In recent years, it has been found that *MAP2K6* may be associated with tumorigenesis and progression [21]. *MAP2K6* may be involved in human tumorigenesis and progression and may be considered a new diagnostic or prognostic biomarker for cancer [22, 23]. Previous studies have shown that *MAP2K6* plays a vital role in cell cycle regulation, transcription, and apoptosis. Parry et al. [15] found significantly higher expression of *MAP2K6* in esophageal, gastric, and colon cancers than in controls using protein blotting and immunofluorescence assays, and overexpression of *MAP2K6* suggests a role in human cancers. It may be a novel diagnostic or prognostic biomarker in these cancers [24–28]. *DHHC8* is localized in mitochondria and is involved in mitochondrial-regulated apoptosis [29]. *DYNLT1* is an integral 14 kDa protein subunit of the large microtubule-based cytoplasmic dynein complex [30]. Wei et al. [31] hypothesized that *DYNLT1* is associated with apoptosis regulation [31]. In addition, *DYNLT1* was previously considered an interaction partner of *REIC/Dkk-3*, inducing apoptosis through its role as a tumor suppressor in various cancer cell lines [32]. *IMMT* is a mitochondrial protein that affects the morphological structure and has a putative impact on mitochondrial function. Although there is little knowledge about the function of *IMMT*, alterations in this marker have been reported in association with different diseases, including Down syndrome, diabetic cardiomyopathy, and Parkinson’s disease [33–37].

This study constructs a prognostic risk score model based on lipid metabolism gene labeling and validates it by survival analysis, ROC curve plotting, risk function assessment, and independent prognostic analysis. We found that *DYNLT1*, *IMMT*, *RAB2A*, and *SLC25A5* were tumor biomarkers to assess the prognosis of BRCA patients, and all of them were high-risk genes, and the parameters indicated

that 4 genes would make the prognosis of BRCA poorer. These results provide new ideas and approaches for developing drugs targeting the energy metabolism of BRCA cells and for the clinical treatment of BRCA.

Abbreviations

abrBRCA:	Breast invasive carcinoma
TCGA:	The Cancer Genome Atlas
GSEA:	Gene set enrichment analysis
GSVA:	Gene set variation analysis
GO:	Gene ontology
KEGG:	Kyoto Encyclopedia of Genes and Genomes
WGCNA:	Weighted correlation network analysis
ROC:	Receiver operating characteristic
AUC:	Area under the ROC curve
TME:	Tumor microenvironment
TNM:	Tumor-node-metastasis
FC:	Fold change.

Data Availability

The datasets generated during this study are available in the TCGA database (<https://portal.gdc.cancer.gov/repository>).

Disclosure

Zhixing Wang and Fan Wang are the co-first authors.

Conflicts of Interest

The authors declare that they have no conflicts of interest.

References

- [1] H. Sung, J. Ferlay, R. L. Siegel, M. Laversanne, and I. Soerjomataram, "Global Cancer Statistics 2020: GLOBOCAN Estimates of Incidence and Mortality Worldwide for 36 Cancers in 185 Countries," *CA: A Cancer Journal for Clinicians*, vol. 71, no. 3, pp. 209–249, 2021.
- [2] F. R. Maxfield, "Plasma membrane microdomains," *Current Opinion in Cell Biology*, vol. 14, no. 4, pp. 483–487, 2002.
- [3] G. Van Meer, "Membranes in motion," *EMBO Reports*, vol. 11, no. 5, pp. 331–333, 2010.
- [4] H. N. Abramson, "The lipogenesis pathway as a cancer target," *Journal of Medicinal Chemistry*, vol. 54, no. 16, pp. 5615–5638, 2011.
- [5] E. Grossi-Paoletti, P. Paoletti, and R. Fumagalli, "Lipids in brain tumors," *Journal of Neurosurgery*, vol. 34, no. 3, pp. 454–455, 1971.
- [6] F. Podo, "Tumour phospholipid metabolism," *NMR in Biomedicine*, vol. 12, no. 7, pp. 413–439, 1999.
- [7] S. Yoon, M. Y. Lee, S. W. Park et al., "Up-regulation of acetyl-CoA carboxylase α and fatty acid synthase by human epidermal growth factor receptor 2 at the translational level in breast cancer cells," *Journal of Biological Chemistry*, vol. 282, no. 36, pp. 26122–26131, 2007.
- [8] M. G. Vander Heiden, L. C. Cantley, and C. B. Thompson, "Understanding the Warburg effect: the metabolic requirements of cell proliferation," *Science*, vol. 324, no. 5930, pp. 1029–1033, 2009.
- [9] C. Cheng, F. Geng, X. Cheng, and D. Guo, "Lipid metabolism reprogramming and its potential targets in cancer," *Cancer Communications*, vol. 38, no. 1, p. 27, 2018.
- [10] H. K. Grosshans, T. T. Fischer, J. A. Steinle, A. L. Brill, and B. E. Ehrlich, "Neuronal Calcium Sensor 1 is up-regulated in response to stress to promote cell survival and motility in cancer cells," *Molecular Oncology*, vol. 14, no. 6, pp. 1134–1151, 2020.
- [11] M. Chidiac, M. Fayyad-Kazan, J. Daher et al., "Apolipoprotein L1 is expressed in papillary thyroid carcinomas," *Pathology, Research & Practice*, vol. 212, no. 7, pp. 631–635, 2016.
- [12] J. Chu, N. Li, and F. Li, "A risk score staging system based on the expression of seven genes predicts the outcome of bladder cancer," *Oncology Letters*, vol. 16, no. 2, pp. 2091–2096, 2018.
- [13] B. Johanneson, S. K. McDonnell, D. M. Karyadi et al., "Family-based association analysis of 42 hereditary prostate cancer families identifies the apolipoprotein L3 region on chromosome 22q12 as a risk locus," *Human Molecular Genetics*, vol. 19, pp. 3852–3862.
- [14] E. Pays, "The function of apolipoproteins L (APOLs): relevance for kidney disease, neurotransmission disorders, cancer and viral infection," *FEBS Journal*, vol. 288, no. 2, pp. 360–381, 2021.
- [15] J. F. O'Toole, L. A. Bruggeman, S. Madhavan, and J. R. Sedor, "The cell biology of APOL1," *Seminars in Nephrology*, vol. 37, no. 6, pp. 538–545, 2017.
- [16] C. L. Cummins, D. H. Volle, Y. Zhang et al., "Liver X receptors regulate adrenal cholesterol balance," *Journal of Clinical Investigation*, vol. 116, no. 7, pp. 1902–1912, 2006.
- [17] F. Fang, D. Li, L. Zhao, Y. Li, T. Zhang, and B. Cui, "Expression of NR1H3 in endometrial carcinoma and its effect on the proliferation of Ishikawa cells in vitro," *OncoTargets and Therapy*, vol. 12, pp. 685–697, Jan 18 2019.
- [18] K. E. Swales, M. Korbonits, R. Carpenter, D. T. Walsh, T. D. Warner, and D. Bishop-Bailey, "The farnesoid X receptor is expressed in breast cancer and regulates apoptosis and aromatase expression," *Cancer Research*, vol. 66, no. 20, pp. 10120–10126, 2006.
- [19] K. Thorsen, T. Schepeler, B. Øster et al., "Tumor-specific usage of alternative transcription start sites in colorectal cancer identified by genome-wide exon array analysis," *BMC Genomics*, vol. 12, no. 1, p. 505, 2011.
- [20] M. M. Motazacker, J. Pirhonen, J. C. van Capelleveen et al., "A loss-of-function variant in OSBPL1A predisposes to low plasma HDL cholesterol levels and impaired cholesterol efflux capacity," *Atherosclerosis*, vol. 252, pp. e259–e260, 2016.
- [21] J. M. Kyriakis and J. Avruch, "Mammalian MAPK signal transduction pathways activated by stress and inflammation: a 10-year update," *Physiological Reviews*, vol. 92, no. 2, pp. 689–737, 2012.
- [22] A. Cuenda, J. M. Lizcano, and J. Lozano, "Editorial: mitogen activated protein kinases," *Frontiers in Cell and Developmental Biology*, vol. 5, p. 80, 2017.
- [23] Z. Li, N. Li, and L. Shen, "MAP2K6 is associated with radiation resistance and adverse prognosis for locally advanced nasopharyngeal carcinoma patients," *Cancer Management and Research*, vol. 10, pp. 6905–6912, 2018.
- [24] G. Remy, A. M. Risco, F. A. Iñesta-Vaquera et al., "Differential activation of p38MAPK isoforms by MKK6 and MKK3," *Cellular Signalling*, vol. 22, no. 4, pp. 660–667, 2010.
- [25] E. Sturchler, D. Feurstein, P. McDonald, and D. Duckett, "Mechanism of oxidative stress-induced ASK1-catalyzed MKK6 phosphorylation," *Biochemistry*, vol. 49, no. 19, pp. 4094–4102, 2010.

- [26] J. Mukai, A. Dhillia, L. J. Drew et al., "Palmitoylation-dependent neurodevelopmental deficits in a mouse model of 22q11 microdeletion," *Nature Neuroscience*, vol. 11, pp. 1302–1310, 2008.
- [27] J. Mukai, H. Liu, R. A. Burt et al., "Evidence that the gene encoding ZDHHC8 contributes to the risk of schizophrenia," *Nature Genetics*, vol. 36, no. 7, pp. 725–731, 2004.
- [28] H. Sudo, A. B. Tsuji, A. Sugyo, Y. Ogawa, M. Sagara, and T. Saga, "ZDHHC8 knockdown enhances radiosensitivity and suppresses tumor growth in a mesothelioma mouse model," *Cancer Science*, vol. 103, no. 2, pp. 203–209, 2012.
- [29] C. Salaun, J. Greaves, and L. H. Chamberlain, "The intracellular dynamic of protein palmitoylation," *Journal of Cell Biology*, vol. 191, no. 7, pp. 1229–1238, 2010.
- [30] R. B. Vallee, R. J. McKenney, and K. M. Ori-McKenney, "Multiple modes of cytoplasmic dynein regulation," *Nature Cell Biology*, vol. 14, no. 3, pp. 224–230, 2012.
- [31] S. Wei, L. Peng, J. Yang et al., "Exosomal transfer of miR-15b-3p enhances tumorigenesis and malignant transformation through the DYNLT1/Caspase-3/Caspase-9 signaling pathway in gastric cancer," *Journal of Experimental & Clinical Cancer Research*, vol. 39, no. 1, p. 32, 2020.
- [32] K. Ochiai, M. Watanabe, H. Ueki et al., "Tumor suppressor REIC/Dkk-3 interacts with the dynein light chain, Tctex-1," *Biochemical and Biophysical Research Communications*, vol. 412, no. 2, pp. 391–395, 2011.
- [33] Y. Hiyoshi, Y. Sato, M. Ichinoe et al., "Prognostic significance of IMMT expression in surgically-resected lung adenocarcinoma," *Thoracic cancer*, vol. 10, no. 11, pp. 2142–2151, 2019.
- [34] G. Bernert, M. Fountoulakis, and G. Lubec, "Manifold decreased protein levels of matrin 3, reduced motor protein HMP and hlark in fetal Down's syndrome brain," *Proteomics*, vol. 2, no. 12, pp. 1752–1757, 2002.
- [35] H. Kajihio, Y. Kajihio, and G. Scita, "Harnessing membrane trafficking to promote cancer spreading and invasion: the case of RAB2A," *Small GTPases*, vol. 9, no. 4, pp. 304–309, 2018.
- [36] M. Aizawa and M. Fukuda, "Small GTPase Rab2B and its specific binding protein golgi-associated Rab2B interactor-like 4 (GARI-L4) regulate Golgi morphology," *Journal of Biological Chemistry*, vol. 290, no. 36, 22261 pages, 2015.
- [37] X. Ni, Y. Ma, H. Cheng et al., "Molecular cloning and characterization of a novel human Rab (Rab2B) gene," *Journal of Human Genetics*, vol. 47, no. 10, pp. 0548–0551, 2002.